

Polychromatic LED Therapy in Burn Healing of Non-diabetic and Diabetic Rats

FAROUK A.H. AL-WATBAN, M.Sc., Ph.D., and BERNARD L. ANDRES, R.M.T., M.T.(A.M.T.)

ABSTRACT

Objective: We determined the effect of polychromatic light-emitting diodes (LED) in burn healing of non-diabetic and streptozotocin-induced diabetic rats. **Background Data:** LEDs were used as the light source for phototherapy. **Materials and Methods:** The polychromatic LED is a cluster of 25 diodes emitting photons at wavelengths of 510–543, 594–599, 626–639, 640–670, and 842–879 nm with 272-mW output power. Age-matched, male Sprague-Dawley rats ($n = 30$) were used. Streptozotocin (70 mg/kg) was used for diabetes induction. Rat weight, hyperglycemia, and glycosuria were monitored for the first 3 days and weekly thereafter. Rats were anesthetized and shaved after 1 week of diabetes. Burn areas of $1.5 \pm .03 \text{ cm}^2$ were created using a metal rod pre-heated up to 600°C that was applied for 2 sec. Diabetic and non-diabetic rats were randomized into the following treatment groups: control, 5, 10, 20, and 30 J/cm^2 . Light treatment commenced after burn infliction and was repeated three times per week. Burn areas were measured daily. **Results:** Burn healing was impaired significantly during diabetes by -46.17% . Polychromatic LED treatment using 5, 10, 20, and 30 J/cm^2 incident doses influenced healing by 6.85%, 4.93%, -4.18% , and -5.42% in the non-diabetic rats; and 73.87%, 76.77%, 60.92%, and 48.77% in the diabetic rats, relative to their controls, respectively. **Conclusion:** The effect of polychromatic LED in non-diabetic rats was insignificant; however, it simulated the trend of stimulation and inhibition seen using low-level lasers. Significant stimulation observed in the diabetic rats demonstrated the usefulness of polychromatic LED in diabetic burn healing.

INTRODUCTION

STUDIES OF LIGHT-EMITTING DIODES (LEDs) as a source of photons for wound healing, pain relief, and other pathologic conditions are emerging. The efficacy of LED use, however, remains to be confirmed. During the last decade, we have determined the efficacy of various laser wavelengths in healing oval full-thickness wounds in the non-diabetic rat. These studies concluded that lasers (with 442, 514, 632.8, 670, 780, 830, and 10,600 nm wavelengths) influenced wound healing.^{1–5} While our studies of the efficacy of various lasers showed biostimulative effects, simultaneous irradiation using several wavelengths was facilitated only with the use of a polychromatic LED array. In this study, we explored the utility of polychromatic LED therapy in the healing of burn wounds in the diabetic and non-diabetic rat.

MATERIALS AND METHODS

Animals

Age-matched, male Sprague-Dawley rats ($n = 30$), weighing 270–367 g, were used in this study. The animals were originally imported from Charles River Co. (U.K.) in 1984. Now, they are bred and provided by the Animal Facility under the Comparative Medicine Department of King Faisal Specialist Hospital and Research Centre. All animal protocols were reviewed and approved by the Animal Care and Use Committee.

Chemical induction of diabetes

Streptozotocin (Sigma, St. Louis, MO), a pancreatic beta-cell toxin, dissolved in sterile NSS was injected peritoneally using a dose of 70 mg/kg. Diabetes was assessed by estimating hyper-

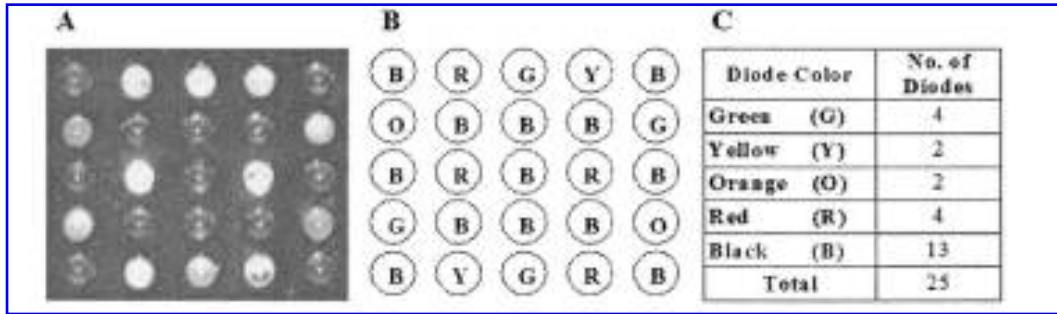


FIG. 1. Polychromatic LED placement and quantity

glycemia and glycosuria. Animals were rejected when blood and urine glucose did not reach 200 mg/dL and four pluses (++++) (≥ 111 mmol/L or ≥ 20 g/L) respectively, after 24 h post-induction together with an increase in weight at 72 h post-induction.

Hyperglycemia, glycosuria, and rat weight

Rat weight, and blood and urine glucose baseline values were determined initially before diabetes induction. Rat weight was monitored with the use of an electronic balance (Ohaus-Voyager, Switzerland). Blood glucose concentration was determined using Lifescan One-Touch II glucometer and strips (Johnson & Johnson Co.) using blood obtained from the tail vein. Multistix 10 SG (Bayer) was used in estimating glycosuria. Blood glucose was evaluated 24 h after diabetes induction; urine glucose was measured at 24, 48, and 72 h after diabetes induction. Final blood glucose concentration was determined at day 21. Urine glucose was monitored weekly for 3 weeks after burn infliction.

Burn wound infliction

Rats were anesthetized with 50 mg/kg ketamine and 20 mg/kg xylocaine. The gluteus maximus region and adjacent area were shaved in a rectangular fashion, to the dimensions of

TABLE 1. POLYCHROMATIC LED WAVELENGTHS

<i>Diode color</i>	<i>Manufacturer's λ specification</i>	<i>Laser laboratory λ measurement</i>
Green	558	510–543
Yellow	587	594–599
Orange	605	626–639
Red	660	640–679
Black	950	842–872

more than 4 cm in width and 5 cm in length, in order to accommodate the light spot from the LED array. This was followed by the application of hair removal lotion, and then the area was sanitized with 70% isopropyl alcohol. Burn wounds of 1.5 ± 0.03 cm² were created using a metal rod heated up to 600°C that was applied for two seconds.

LED data and treatment parameters

The 25-LED array (Pain X2000, model 2500-W, Diomedics, Inc.) was used for the polychromatic LED therapy. The LEDs

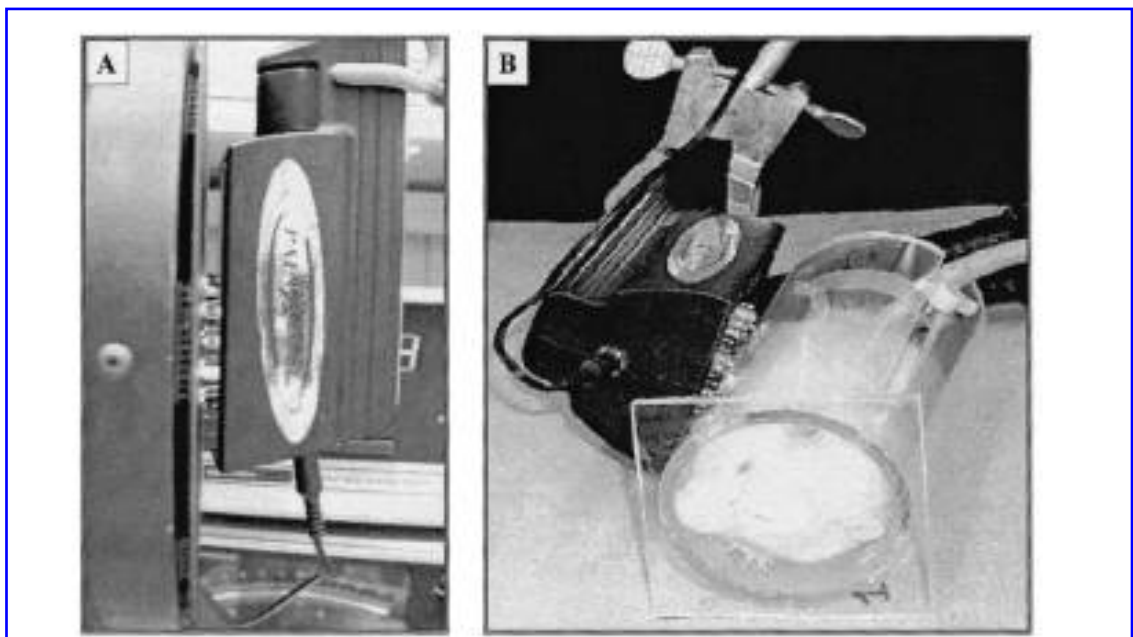


FIG. 2. Polychromatic LED power output measurement and animal treatment.

TABLE 2. POLYCHROMATIC LED OUTPUT POWER

<i>Polychromatic LED output-power (mW)</i>	
Manufacturer's original specification	1,875 mW
Change made after verification ^a	441.3 mW
KFSH&RC laser laboratory measurement ^b	272 mW

^aPersonal communication.

^bPower output value used for dose calculation.

TABLE 3. POLYCHROMATIC LED TREATMENT PARAMETERS

<i>Dose</i>	<i>Treatment time</i>
Control	0
5 J/cm ²	6 min, 7 sec
10 J/cm ²	12 min, 15 sec
20 J/cm ²	24 min, 30 sec
30 J/cm ²	36 min, 46 sec

were mounted and distributed in a 20-cm² area (Fig. 1A,B). Light emissions of 510–543 nm (G = green diode), 594–599 nm (Y = yellow diode), 626–639 nm (O = orange diode), 640–670 nm (R = red diode), and 842–872 nm (B = black diode) from the LED array were determined using a monochromator and power meter (Metrologic™) (Fig. 1B,C and Table 1). The power output was measured at 272 mW using a power meter (Scientech™), with 8-inch-diameter probe (Fig. 2A and Table 2). The LED array's power density was 13.6 mW/cm² for the treated area of 20 cm². Non-diabetic and diabetic rats were treated according to the computed treatment time for each treatment group: control, 5 J/cm², 10 J/cm², 20 J/cm², and 30 J/cm² (Table 3). Immediately after burn infliction, the experimental animals were placed in Plexiglas restriction cages (Fig. 2B). Light treatments were performed three times a week for 3 consecutive weeks.

The power density (mW/cm²) is the dose rate of the light. This is calculated as the output power in mW, divided by the LED array spot size in cm². The dose (J/cm²) is the energy density of the LED. This is calculated by using power density in watts (W), multiplied by treatment time in seconds.

Analysis

Burn wounds were measured daily using a caliper. Digital pictures (Kodak DC290) were taken every 7 days commencing on the day of burn infliction. Burn areas derived from daily caliper measurements were plotted, and a linear-fit was used to determine the value of the slope and the trend (Fig. 3A). Burn healing acceleration, deceleration, and zero bio-activation were dependent on the relative burn healing (%) value that was obtained. A positive value signifies acceleration, a negative value signifies deceleration, and a value of zero signifies zero-bioactivation. Our computation (Fig. 3A) used the slope values of the treated group and control. Relative burn healing was computed using the following formula:

$$\text{Relative burn healing (\%)} = \frac{(\text{Slope treated} - \text{Slope control})}{\text{Slope control}} \times 100$$

This method of calculation evolved from calculations used in previous publications,¹⁻⁵ done for simplicity and adaptability in the research and clinical settings. For review and comparison, previous methods of calculation are presented in Figure 3B,C.

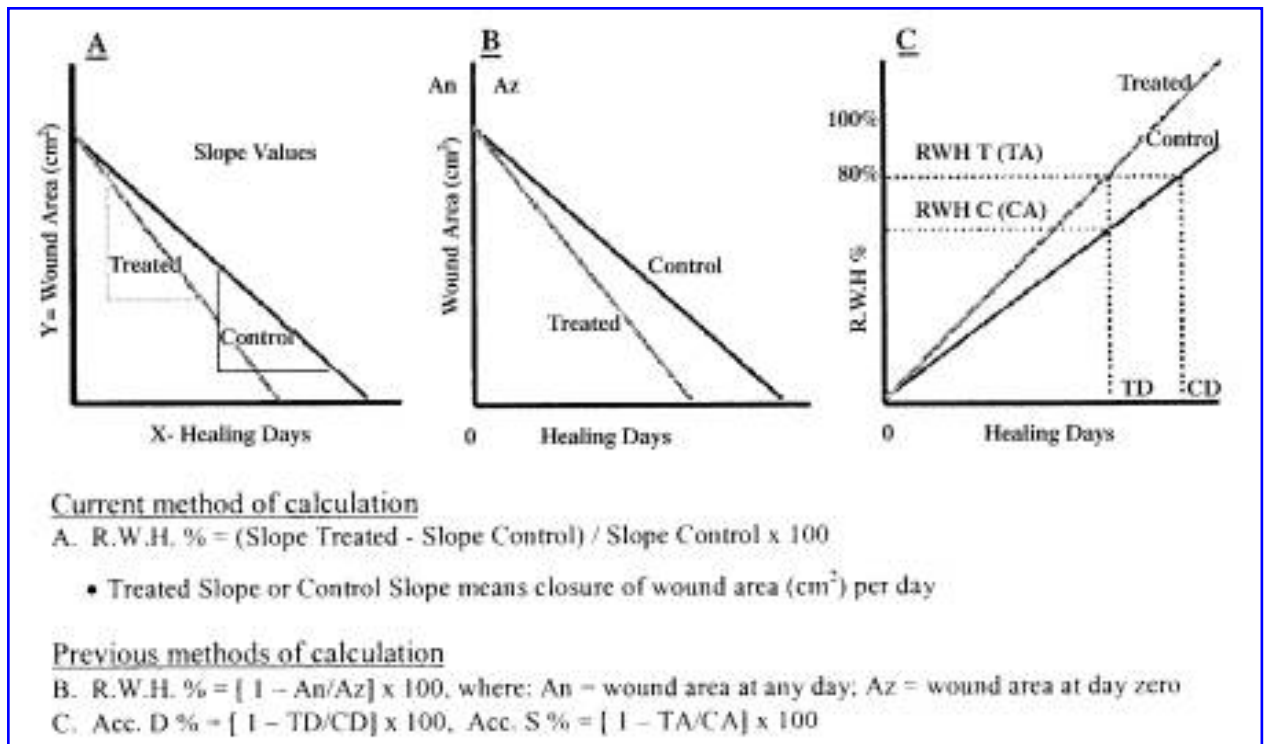


FIG. 3. Current and previous methods of calculation in wound healing experiments.

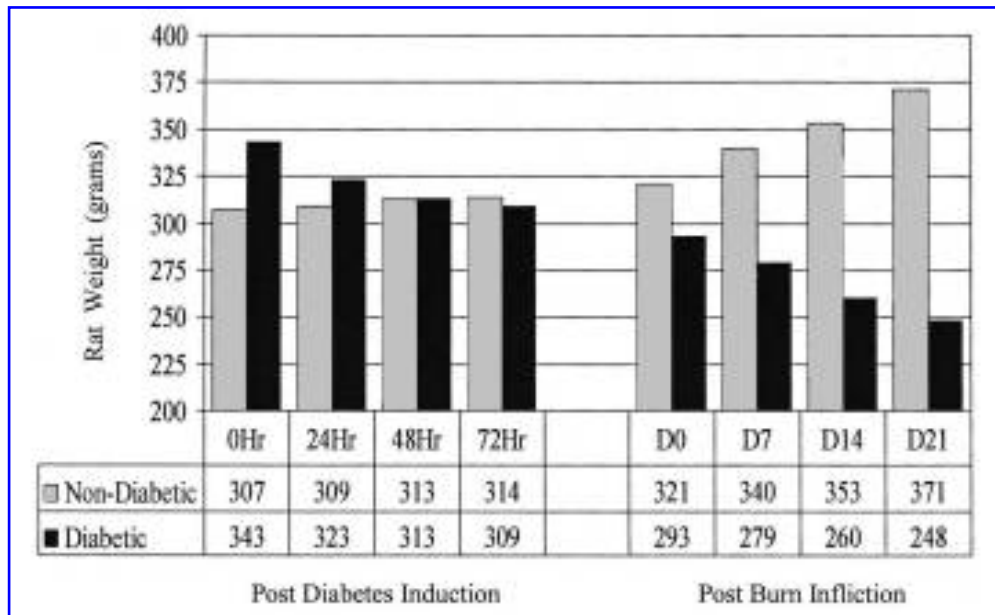


FIG. 4. Non-diabetic and diabetic rat weight after diabetes induction and during burn healing.

RESULTS

Table 1 shows the measured wavelength emissions of each diode. Discrepancies in the wavelength emissions and output power were noticed when compared with the manufacturer's product specification. Figure 1C shows the number of diodes mounted in the LED array, and Figure 2B shows the manner in which the rats were treated. The total output power of 272 mW was determined (Table 2) and used as the basis for light dose and treatment time calculations (Table 3).

Figure 4 shows that the non-diabetic rats gained weight continuously during the course of the study. The non-diabetic rats gained 2.33 g/day before burn infliction and 2.38 g/day after burn infliction. As opposed to the weight gain in the non-diabetic rats, weight loss was manifested by the diabetic rats at a rate of 11.33 g/day during the first 3 days post-diabetes induction and 2.14 g/day after burn infliction. The non-diabetic rats gained weight by 20.85% and the diabetic rats lost weight by 27.69% during the 4-week duration of the study.

TABLE 4. WHOLE BLOOD AND URINE GLUCOSE PROFILES OF NON-DIABETIC BURN TREATMENT GROUPS

<i>Whole Blood Glucose Determination</i>			
<i>Groups</i>	<i>Baseline values</i>	<i>After 24 h</i>	<i>3rd week post burn</i>
Control	56 ± 4 mg/dL	60 ± 5 mg/dL	60 ± 8 mg/dL
5 J	50 ± 5 mg/dL	57 ± 8 mg/dL	63 ± 5 mg/dL
10 J	59 ± 7 mg/dL	65 ± 6 mg/dL	56 ± 5 mg/dL
20 J	48 ± 4 mg/dL	60 ± 4 mg/dL	60 ± 7 mg/dL
30 J	56 ± 8 mg/dL	58 ± 5 mg/dL	60 ± 4 mg/dL

<i>Urine Glucose Determination</i>					
<i>Groups</i>	<i>Baseline values</i>	<i>Burning day (day 0)</i>	<i>1st week post burn</i>	<i>2nd week post burn</i>	<i>3rd week post burn</i>
Control	(-)	(-)	(-)	(-)	(-)
5 J	(-)	(-)	(-)	(-)	(-)
10 J	(-)	(-)	(-)	(-)	(-)
20 J	(-)	(-)	(-)	(-)	(-)
30 J	(-)	(-)	(-)	(-)	(-)

TABLE 5. WHOLE BLOOD AND URINE GLUCOSE PROFILES OF DIABETIC BURN TREATMENT GROUPS

<i>Whole Blood Glucose Determination</i>			
<i>Groups</i>	<i>Pre diabetes induction</i>	<i>24 h post induction</i>	<i>Day 21 final glucose</i>
Control	55 ± 5 mg/dL	317 ± 15 mg/dL	345 ± 30 mg/dL
5 J	53 ± 3 mg/dL	291 ± 18 mg/dL	361 ± 25 mg/dL
10 J	55 ± 4 mg/dL	273 ± 26 mg/dL	358 ± 33 mg/dL
20 J	69 ± 7 mg/dL	332 ± 30 mg/dL	322 ± 20 mg/dL
30 J	60 ± 5 mg/dL	260 ± 25 mg/dL	365 ± 28 mg/dL

<i>Urine Glucose Determination</i>					
<i>Groups</i>	<i>Pre diabetes induction</i>	<i>Burning day (day 0)</i>	<i>1st week post burn</i>	<i>2nd week post burn</i>	<i>3rd week post burn</i>
Control	(-)	(++++)	(++++)	(++++)	(++++)
5 J	(-)	(++++)	(++++)	(++++)	(++++)
10 J	(-)	(++++)	(++++)	(++++)	(++++)
20 J	(-)	(++++)	(++++)	(++++)	(++++)
30 J	(-)	(++++)	(++++)	(++++)	(++++)

Tables 4 and 5 show the blood and urine glucose profiles of the non-diabetic and diabetic rats, respectively. Loss of weight, hyperglycemia, glycosuria, and polyuria, as observed in the diabetic rats during the course of the study, were indicative of uncontrolled diabetes.

Figure 5 compares the healing of oval full-thickness burn wounds in the diabetic and non-diabetic rat. The diabetic oval

full-thickness wound shows lesser bleeding and delayed wound contraction at days 0 and 7 (Fig. 5A), respectively. The diabetic burn wound healing was delayed significantly (Fig. 5B) when compared to the healing of the non-diabetic burn and the healing of both the non-diabetic and diabetic oval full-thickness wounds.

Figures 6 and 7 show representative pictures of each treatment group, including the controls. In Figure 6, insignificant

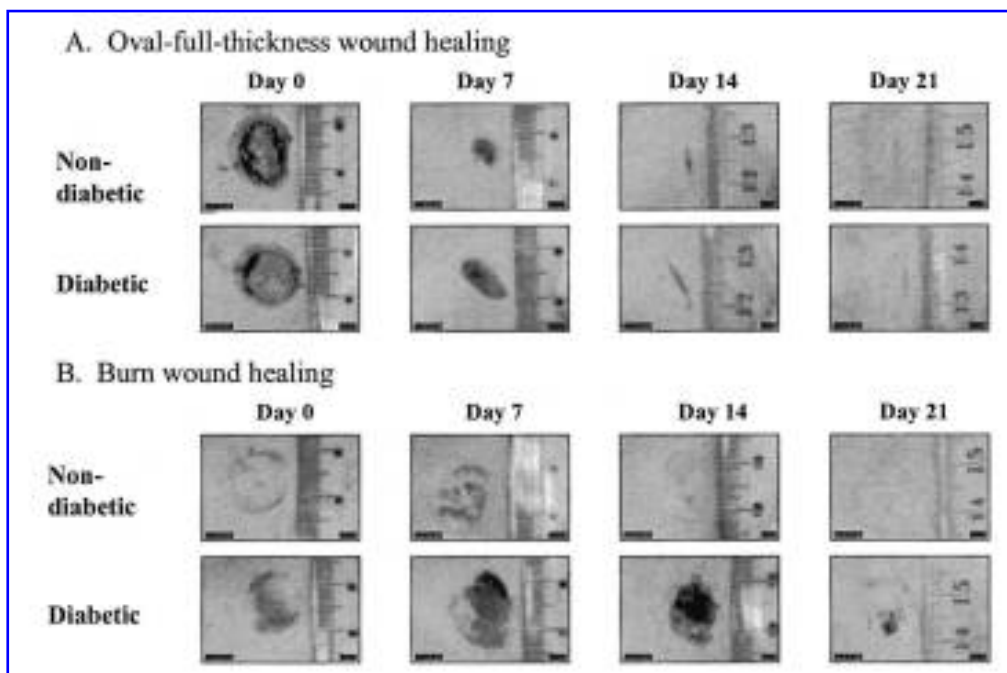


FIG. 5. Wound healing comparison of non-diabetic and diabetic rat.

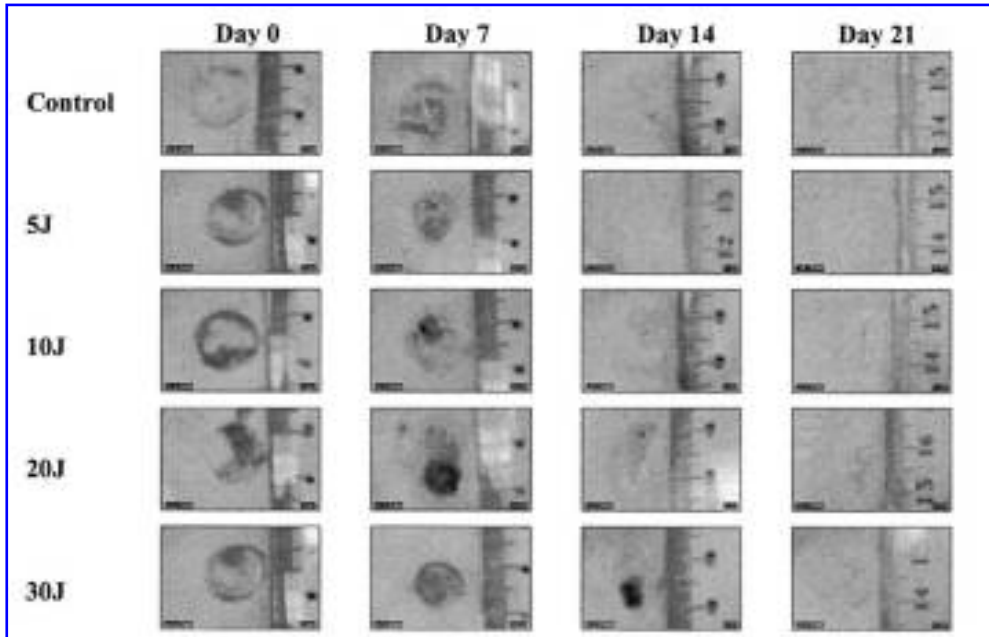


FIG. 6. Polychromatic LED therapy of burn in non-diabetic rats. Treatment schedule: 3 times per week.

burn healing acceleration was evident at 5 and 10 J/cm², while insignificant inhibition was seen at 20 and 30 J/cm². In Figure 7, one can see the efficacy of polychromatic LEDs in decreasing the healing delay caused by diabetes by all the doses used.

Figure 8 shows the delayed and prolonged inflammatory response in the diabetic control rats, as evidenced by the increased area of burn defect at days 1–9 compared to the non-diabetic rats at days 1–6.

Figure 9 shows the relative burn healing (percentage) of non-diabetic and diabetic rats when compared to their corresponding controls. The non-diabetic rats were stimulated at the doses of 5 and 10 J/cm² by 6.65% and 4.93%, and inhibited at 20 and 30 J/cm² by -4.18% and -5.42%, respectively. The diabetic rats were stimulated at 5, 10, 20, and 30 J/cm² by 73.87%, 76.77%, 60.92%, and 48.77%, respectively.

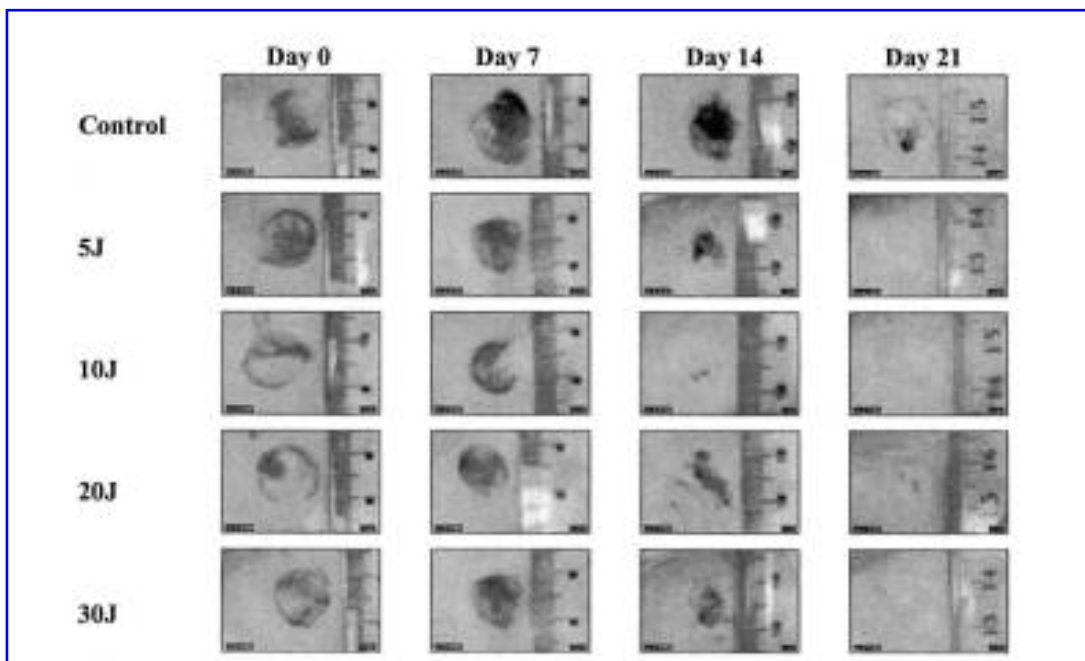


FIG. 7. Polychromatic LED therapy of burn in diabetic rats. Treatment schedule: 3 times per week.

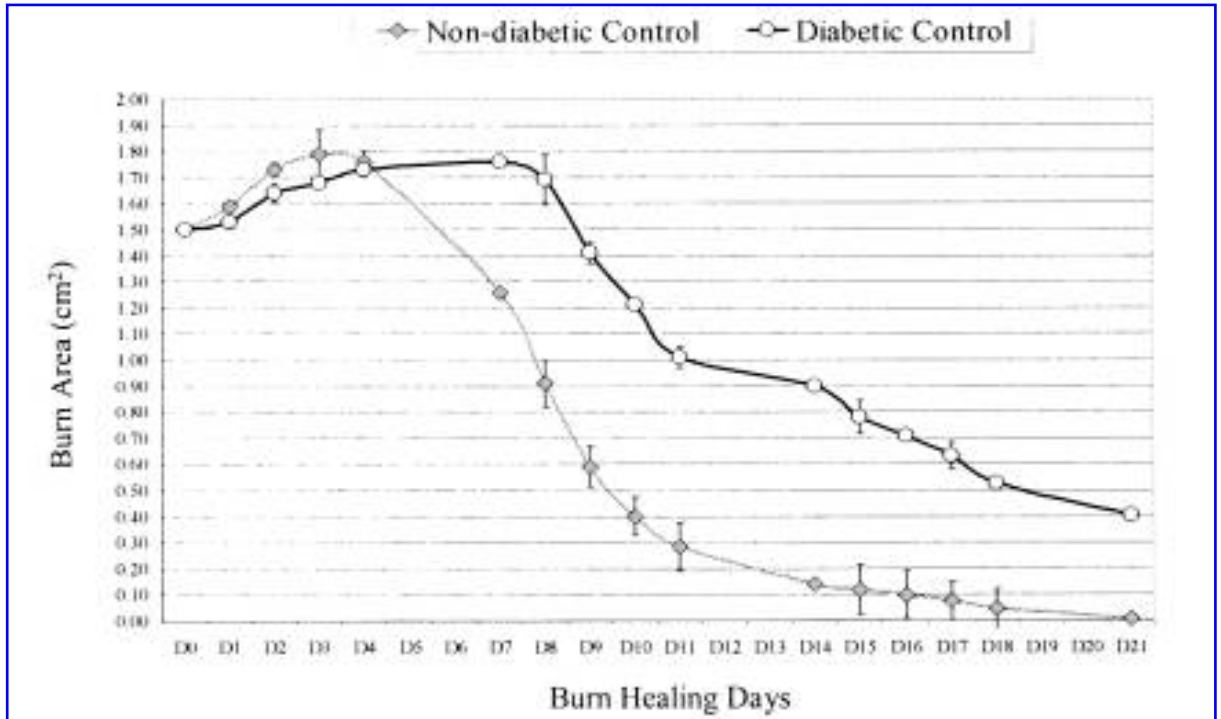


FIG. 8. Burn healing in the non-diabetic and diabetic controls.

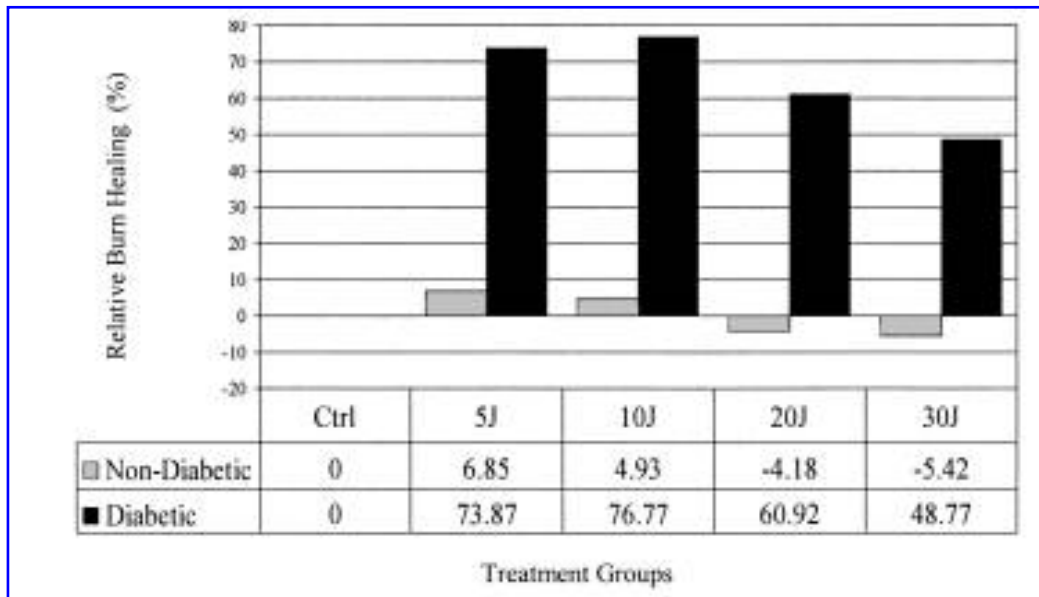


FIG. 9. Burn healing in the non-diabetic and diabetic rat after polychromatic LED therapy (relative to their respective controls).

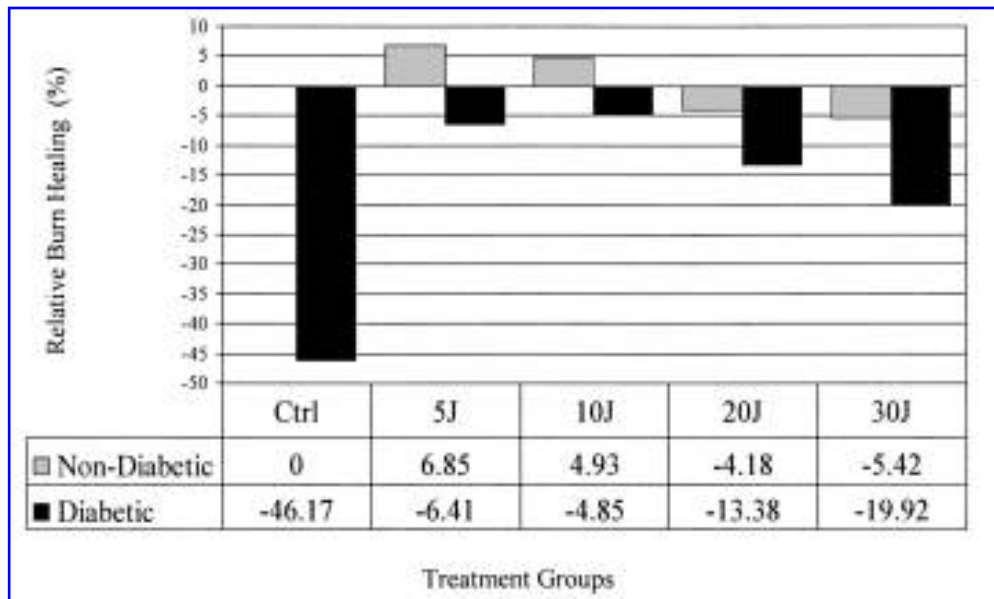


FIG. 10. Burn healing in the non-diabetic and diabetic rat after polychromatic LED therapy (relative to the non-diabetic control).

Figure 10 compares the relative burn healing (percentage) delay of the diabetic to the non-diabetic rat. When the diabetic control was compared to the non-diabetic control, a burn healing delay of -46.17% was exhibited during diabetes. The slope value of the non-diabetic control was used as the denominator to determine the effect of polychromatic LED treatment in the diabetics relative to the non-diabetic rats. LED treatment at 5, 10, 20, and 30 J/cm² reduced diabetic burn healing impairment to -6.41% , -4.85% , -13.38% , and -19.92% , respectively, from -46.17% .

DISCUSSION

Our LED treatment used an array of 25 diodes (Fig. 1A) covering an area of 20 cm² and a similar area was shaved to expose the rat skin to the light treatment. The LED array was positioned centrally and directly into the burn so that it would not touch the Plexiglas, as heat is generated by the diodes during prolonged exposure (Fig. 2B). The LED array distance of 1 mm to the Plexiglas was observed during treatment. Similar distance of 1 mm from the LED array to the probe was also maintained during power output measurement (Fig. 2A) to minimize power loss due to beam divergence. In our previous studies, we determined power loss from Plexiglas reflection using various laser wavelengths.⁴ However, the beam divergence inherent in LED does not allow Plexiglas power loss determination with our current instrumentation.

The polychromatic LED wavelength emissions were determined with the use of a monochromator and power meter. The power meter probe was carefully aligned to the exit slit of the monochromator, and each of the diodes carefully aligned to the entrance slit. Wavelength emissions were scanned by turning the monochromator dial. Discrepancies in the wavelength emissions were noticed when compared to the manufacturer's

data (Table 1). Our wavelength determination confirmed the broad range of wavelengths innate to LED. This disparity as compared to the manufacturer's specification reflects the quality of the LEDs. Measures to augment quality are necessary, especially when LEDs are to be used for patient care.

The total output power of the LED array was determined using a power meter with an 8-inch-diameter probe (Fig. 2A). The result of our measurement was 272 mW, which is 38% less than the manufacturer's verified power output of 441.3 mW (private correspondence) and 85% less than what was in the manufacturer's original specification of 1,875 mW. The output power discrepancies reflect the manner with which the diode power was measured. The manufacturer measured the diode output power individually before installation, while we measured ours with the diodes already mounted, which may have accounted for the power loss of 38% (or the loss of 85%). It is worth mentioning that, since LED emissions are divergent, the power output falls dramatically as the distance from the source to the power meter probe is increased; so, the distance of 1 mm was maintained during power measurement and LED treatment (Fig. 2A,B). Our dose computation was based on the actual power measurement derived in our laboratory (Tables 2 and 3). The wavelength and power output measurements were done to determine the actual technical performance of the LED array and to properly define our method.

We have monitored the animals' weight (Fig. 4), and blood and urine glucose (Tables 4 and 5) in both the non-diabetic and diabetic rats to ascertain their metabolic state during the course of the study. Weight loss in the diabetic rat of 11.33 g/day, plus 4 (++++) urine glucose during the first 3 days, elevation of blood glucose concentrations to over 200 mg/dL immediately after 24 h post-diabetes inception were indicative of a successful diabetes induction. That diabetic rats lost weight by an average of 27.69%, with final blood glucose concentrations of over 300 mg/dL during week 3 after burn infliction manifested

the condition of uncontrolled diabetes. On the other hand, the non-diabetic rats gained weight by 20.85% with normal blood glucose values and negative urine glucose during the course of the study.

Figure 5A,B shows differences in the healing of non-diabetic and diabetic controls at days 7, 14, and 21 in the oval full-thickness wound and burn wound model. The non-diabetic controls were almost completely healed at day 14. At days 14 and 21, the diabetic oval full-thickness and diabetic burn wound model have wound areas still left unhealed, respectively. The oval full-thickness wound in the non-diabetic rat had the tendency to bleed more, as compared to its diabetic counterpart. While this defect is not evident in the burn model, it is indirectly manifested through the healing delay observed in the diabetic rats (Fig. 7) when compared to the non-diabetic rats (Fig. 6).

The delayed and prolonged inflammatory response in the diabetic burn from day 1 to day 9, compared to the non-diabetic burn from day 1 to day 6 (Fig. 8) was deduced from the increase in burn area. This suggests that burn-healing impairment in the diabetic rats may in part be due to the delay and prolongation of the inflammatory response. The prolongation of inflammatory response was consistent with the findings of Wetzler et al.⁶ that macrophage-inflammatory protein-2/mRNA together with the macrophage-chemoattractant-protein-1/mRNA expressions were extended and directly associated with sustained infiltration, but with different localization of PMN and macrophages in the diabetic wound. It was also found out by Rendell et al.⁷ that skin blood flow early in the streptozotocin-induced diabetic rats was decreased by 30–40% as a function of time paralleling the increase in glycated hemoglobin. This defect in microcirculation leads to the delay of inflammatory cells reaching the burn site, aggravated by the blocking of capillaries (by coagulated proteins and cellular debris) that needs to be cleared out. The delayed and prolonged inflammatory responses consequently delay angiogenesis, fibroplasia, and reparative collagen accumulation in addition to the decreased delivery of nutrients and oxygen to initiate and sustain the reparatory process.

Unlike the healing of oval full-thickness wounds, where wound contraction, which causes a dramatic reduction of the wound area, is a major feature (Fig. 5A, day 7), burn wounds heal through the generation of epithelial cover, which gradually seals off the skin defect (Fig. 5B, days 7–21). In the non-diabetic rat, the exfoliation of burnt skin and noticeable re-epithelialization were evident during the first week, except for the 30 J/cm² treatment group, where burnt skin was still in place (Fig. 7). During the second-week, complete closure was seen for the 5 and 10 J/cm² treatments; the 20 J/cm² treatment barely delayed re-epithelialization, while the 30 J/cm² treatment delayed it markedly. All the treatment groups exhibited complete burn closure during the third week; however, differences in macroscopic appearance of the newly repaired tissues were evident. While the relative burn healing of 6.65% using 5 J/cm² was insignificant, the quality of healing was macroscopically better.

Burn healing in the diabetic control was delayed by –46.17% (Figs. 5B and 10). In the oval full-thickness wound (Fig. 5A), the diabetic wound did not contract as much as wound in the non-diabetic rat did. This signifies a defect and/or delay in fibroblast proliferation and maturation, both of which are responsible for wound contraction in the oval full-thickness

wound. The diabetic burn healing delays were minimized to –6.41%, –4.85%, –13.38%, and –19.92% after the application of polychromatic LED at 5, 10, 20, and 30 J/cm² light doses, respectively, despite the delay in re-epithelialization after a burn wound.

A study by Tachihara et al.⁸ has demonstrated that coherent and non-coherent low-intensity light induces vasodilation *in vivo*, while Lanzafame et al.,⁹ using the NASA LED treatment (7 J/cm²) showed increase NO production in the wound through the analysis of total nitrate and nitrites as NO markers. These studies imply that, indeed, light treatments influence microcirculation. The up-regulation of NO, a vaso-relaxant, during light treatment confirms our assumption that light treatment enhances diabetic burn closure through its effect on microcirculation, aside from other known photo-biological effects such as increased cellular respiration and ATP synthesis in the mitochondria, which fuels the metabolic repair processes.

However, when NO is produced in excess, to combine with super-oxide anions to form peroxynitrite, it will overactivate the poly-ADP-ribose polymerase depleting the cellular stores of its substrate, NAD⁺, which will lead to “cellular energetic catastrophe,” resulting in cell death.¹⁰ Nitric oxide may also function as an anti-inflammatory mediator.¹¹ These occurrences may be related to the observed inhibitory effect in the non-diabetic rat and the diminished burn healing efficacy in the diabetic rat at light doses of 20 and 30 J/cm².

Figures 9 and 10 are graphic representations of the effect of polychromatic LED treatment in the non-diabetic and diabetic rats. These figures show that the effect of polychromatic LED on burn wound closure was dose dependent. The doses of 5 and 10 J/cm² in the non-diabetic rat accelerated wound closure, while 20 and 30 J/cm² were inhibitory. In the diabetic rat, marked burn healing acceleration was exhibited in all the light doses used, with 10 > 5 > 20 > 30 J/cm² in efficacy (Fig. 9). The light doses of 5 and 10 J/cm² gave the best healing acceleration incidental to the NASA LED dose of 7 J/cm², which almost doubled the NO and collagen production during the first week of healing. While the NASA LED experiment was done on non-diabetic rats, our results show that the diabetic rats appear to benefit more from polychromatic LED treatment in burn healing than the non-diabetic rats. Our *in vitro* studies have also demonstrated that cells cultured in nutrient-deficient medium benefited more from light treatment than cells cultured in optimum culture medium.^{12,13}

CONCLUSION

This study demonstrated that polychromatic LED therapy affects burn healing in a dose-dependent manner. The doses of 5 and 10 J/cm² were barely effective in accelerating burn healing in the non-diabetic rats, while they were outstandingly effective at 5, 10, 20, and 30 J/cm² in the diabetic rats. The effect of light treatment on NO synthesis (enhancing vasodilation) and its effect on inflammatory cells are areas that need to be studied, particularly in the diabetic burn model, where the defect in microcirculation and the delay and prolonged inflammatory response are perceived to contribute to the impairment of burn healing in diabetics. The use of polychromatic LED as

a light source in phototherapy is in its infancy, so stricter guidelines to improve LED manufacturing standards and quality control should be imposed. Further studies that are directed at finding the optimum wavelength and light dose combinations need to be done to augment efficacy, concurrent with filling gaps in our knowledge about the mechanisms of its effect.

ACKNOWLEDGMENTS

We acknowledge the support extended by the Research Centre, King Faisal Specialist Hospital and Research Centre, and our Secretary, Luisa M. Tiongco.

REFERENCES

1. Al-Watban, F.A.H., and Zhang, X.Y. (1994). The dosimetry and response of wound healing to He-Ne laser. *Laser Ther.* 6, 119–124.
2. Al-Watban, F.A.H., Zhang, X.Y. (1995). Stimulative and inhibitory effects of low incident levels of argon laser energy on wound healing. *Laser Ther.* 7, 11–18.
3. Al-Watban, F.A.H., and Zhang, X.Y. (1996). Comparison of the effects of laser therapy on wound healing using different laser wavelengths. *Laser Ther.* 8, 127–135.
4. Al-Watban, F.A.H., A.M. Verga Scheggi, S. Martellucci, et al. (1996). Therapeutic lasers effectiveness and dosimetry, in: *Biomedical Optical Instrumentation and Laser-Assisted Biotechnology*. A.M. Verga Scheggi, et al. (eds.). Amsterdam: Kluwer Academic Publishers, pp. 171–183.
5. Al-Watban, F.A.H., and Zhang, X.Y. (1999). The acceleration of wound healing is not attributed to laser skin transmission. *Laser Ther.* 11, 6–10.
6. Wetzler, C., Kampfer, H., Stallmeyer, B., et al. (2000). Large and sustained induction of chemokines during impaired wound healing in the genetically diabetic mouse: prolonged persistence of neutrophils and macrophages during the late phase of repair. *J. Invest. Derm.* 115, 245–253.
7. Rendell, M.S., Kelly, S.T., Finney, D., et al. (1991). Decreased skin blood flow early in the course of streptozotocin-induced diabetes mellitus in the rat. *Diabetologia* 36, 907–911.
8. Tachihara, R., Farinelli, W.A., and Rox Anderson, R. (2002). Low-intensity light-induced vasodilation *in vivo*. *Lasers Surg. Med.* S14, 11.
9. Lanzafame, R.J., Stadler, I., and Whelan, H.T. (2002). NASA LED photoradiation influences nitric oxide and collagen production in wounded rats. *Lasers Surg. Med.* S14, 12.
10. Virag, L., Szabo, E., Bakondi, E., et al. (2002). Nitric oxide-peroxynitrite-poly(ADP-ribose) polymerase pathway in the skin. *Exp. Dermatol.* 11, 189–202.
11. Molainen, E., Whittle, B., and Moncada, S. (1999). Nitric oxide as factor in inflammation, in: *Inflammation: Basic Principles and Clinical Correlates*. J.I. Gallin, R. Snyderman, D.T. Fearon, et al. (eds.). Philadelphia: Lippincott Williams & Wilkins, pp. 787–800.
12. Al-Watban, F.A.H., and Andres, B.L. (2000). Effect of He-Ne laser (632.8 nm) and Polygen™ on CHO cells. *J. Clin. Laser Med. Surg.* 18, 145–150.
13. Al-Watban, F.A.H., and Andres, B.L. (2001). Effect of He-Ne laser (632.8 nm) and Solcoseryl™ *in vitro*. *Lasers Med. Sci.* 16, 267–275.

Address reprint requests to:

Farouk A.H. Al-Watban, M.Sc., Ph.D.

Laser Medicine Research Section

Biological and Medical Research Department, MBC-03/106

P.O. Box 3354

Riyadh-11211, Saudi Arabia

E-mail: Watban@KFSHRC.EDU.SA